



LAWRENCE  
LIVERMORE  
NATIONAL  
LABORATORY

# Application of solution techniques to rapid growth of organic crystals

N. Zaitseva, L. Carman, A. Glenn, J. Newby, M. Faust,  
S. Hamel, N. Cherepy, S. Payne

July 19, 2010

Journal of Crystal Growth

## **Disclaimer**

---

This document was prepared as an account of work sponsored by an agency of the United States government. Neither the United States government nor Lawrence Livermore National Security, LLC, nor any of their employees makes any warranty, expressed or implied, or assumes any legal liability or responsibility for the accuracy, completeness, or usefulness of any information, apparatus, product, or process disclosed, or represents that its use would not infringe privately owned rights. Reference herein to any specific commercial product, process, or service by trade name, trademark, manufacturer, or otherwise does not necessarily constitute or imply its endorsement, recommendation, or favoring by the United States government or Lawrence Livermore National Security, LLC. The views and opinions of authors expressed herein do not necessarily state or reflect those of the United States government or Lawrence Livermore National Security, LLC, and shall not be used for advertising or product endorsement purposes.

# **Application of solution techniques to rapid growth of organic crystals**

Natalia Zaitseva, Leslie Carman, Andrew Glenn, Jason Newby, Michelle Faust, Sebastien Hamel, Nerine Cherepy, and Stephen Payne

*Lawrence Livermore National Laboratory, 7000 East Avenue, Livermore, California, 94551*

## **Abstract**

Single crystals of a pure hydrocarbon, 1,3,5-triphenylbenzene, with properties suitable for high-energy neutron detection were grown from toluene solutions using slow evaporation and temperature reduction methods with growth rates up to 10 mm/day. Application of the rapid growth technique developed earlier for growth of large water-soluble crystals shows that crystals of aromatic compounds can be successfully grown from solutions in large volumes required for their application as scintillator materials for radiation detection.

## **1. Introduction**

Low-temperature solution growth is the simplest and in many cases the least expensive method for production of optical crystals. Historically, it was probably the first and the most widely used technique to produce artificial crystals for many applications, such as mass crystallization [1], production of pharmaceuticals [2], or growth of relatively small crystals for crystallographic and other physical studies [3]. However, its use for growth of large, commercially important single crystals has been very much limited to a few inorganic water-soluble materials, examples of which include Rochelle salt, triglycine sulphate, or potassium dihydrogenphosphate (KDP). For organic crystals, not soluble in aqueous solutions, the preference has been given to alternative methods, among which the Bridgman technique is the most common. Limited application of solution growth methods to pure organic systems might be

explained by various reasons, such as difficulties in handling and purification of organic compounds and solvents, or, probably the most important, much slower speeds of traditional solution growth in comparison with growth rates of higher-temperature methods from melts. Modern availability of commercially produced high-purity organic solvents and recent development of accelerated techniques for solution growth [5-7] enables wider variations of growth methods to produce crystals of different materials. When large volumes of single crystal materials are needed for certain applications, solution growth methods may offer an advantage of easier scaling-up processes. For organic crystals, one of such application relates to their use in radiation detection devices that deploy scintillation properties of aromatic materials for high-energy neutron detection. The present paper describes growth of relatively large single crystals of a pure hydrocarbon 1,3,5-triphenylbenzene,  $(C_6H_5)_3C_6H_3$ , which is the first in a group of new materials found to have promising properties for potential application in high-energy neutron detection. Crystals were grown from toluene solutions using a method earlier developed for growth of large water-soluble crystals [8]. In addition to practical purposes of obtaining a new material suitable for neutron detection, the subject of work was consideration of similarities and differences between aqueous and organic systems that might be useful in solution growth of other organic crystals.

## **2. Materials and characterization techniques.**

1,3,5-triphenylbenzene is available for purchase from many companies (Aldrich, Alfa Aesar, Acros Organics and TCI America). Independent of the listed purity (from 97 to 99%), all commercial batches had light yellow color that became more intense upon dissolution and

heating. To purify the material, initial powders were first washed in acetone by stirring in a closed vessel at room temperature, and then re-crystallized from toluene 4-6 times until the precipitating crystals became completely colorless. Anhydrous toluene (Aldrich, 99.8%) was used for the preparation of the final growth solutions.

Neutron detection properties of grown crystals were evaluated using the pulse shape discrimination (PSD) technique which allows for the separation of the scintillation pulses produced by neutron and gamma events *via* the relative increase in delayed light for neutron stimulations [9,10]. The measurements were performed using a  $^{252}\text{Cf}$  source shielded with five cm of lead, which reduced the gamma rates to the same order as neutrons, to irradiate crystals coupled to an R6231-S Hamamatsu photomultiplier tube (PMT). The signals collected at the PMT anode were recorded using a high-resolution waveform CompuScope 14200 digitizer with a sampling rate of 200MS/s, for offline analysis. The ability of crystals to discriminate between the neutrons and gamma rays emitted from the  $^{252}\text{Cf}$  source was evaluated using the  $Q_{Tail}/Q_{Total}$  PSD discriminate. The waveforms were numerically integrated over two time intervals:  $\Delta t_{Total}$  and a subinterval  $\Delta t_{Tail}$ , corresponding to the total charge and the delayed component of the signal respectively. The value of the ratio of charge  $R=Q_{Tail}/Q_{Total}$  for the two time intervals indicate whether the considered event was produced by a neutron (high R value) or a gamma ray (small R value). The time gates used for PSD measurements are optimized to maximize FOMs for each material. The  $\Delta t_{Tail}$  gates began at 75 and 140 ns after the pulse peak for stilbene and 1,3,5-triphenylbenzene respectively and extended to 1750 ns after the pulse peak. We note that R is much more sensitive to the start time of  $\Delta t_{Tail}$  as most of the delayed emission occurs in roughly the first 500 ns. Photoluminescence (PL) spectra were measured with UV excitation using a commercial Fluoromax-2 spectrometer. The scintillation light yield of the crystals was

evaluated from the emission spectra acquired under beta-radiation excitation using a  $^{90}\text{Sr}/^{90}\text{Y}$  source, in comparison with two standard inorganic crystals: BGO and  $\text{BaF}_2$ .

### **3. Crystal growth and properties.**

#### ***3.1. Small crystal growth by evaporation***

Initial crystals of 1,3,5 triphenylbenzene (3-PB) used for the first evaluation of their properties were grown using slow evaporation technique. As described previously [11], nicely faceted individual crystals sufficient for x-ray diffraction (XRD) studies could freely form upon slow evaporation of solvent at room temperature. The best of such small crystals were selected under microscopic examination as seeds for growth of larger crystals. Since no solubility data were available for growth of the first crystals, initial solutions were prepared by placing excessive amounts of the solid powder in toluene. The solutions were allowed to stir in sealed jars at room temperature for a few days to reach saturation.

Although the slow evaporation method seems easy, it is still not a trivial task to obtain a relatively large, cm-scale, single crystal by its application. The main obstacle in this task is spontaneous nucleation that leads to the uncontrollable precipitation of multiple crystals causing defect formation and limitations in crystal size. The problem is especially pronounced when growth is conducted from volatile organic solvents like toluene. To diminish the negative effect of these phenomena, a saturated solution of 3-PB was carefully transferred through filtration into a separate vessel with a lid containing a small hole in its middle. With the hole sealed, the solution was overheated 15-20°C above the saturation (room) temperature and then allowed to cool. The overheating of the solution without evaporation helped to break large crystalline

aggregates, substantially increasing the stability of the solutions to spontaneous nucleation [12]. Cooling of the sealed solution promoted condensation on the internal walls of the crystallization vessel, preventing future nucleation on the dry surfaces. The sealed hole was opened only a few degrees above room temperature for the introduction of a small seed simply dropped to the middle of the jar bottom. The slight dissolution of the seed was necessary to remove crystalline dust and defective surfaces before the solution reached the saturation point and growth proceeded by slow evaporation. Variation in the hole size was used to control the evaporation and growth rates that typically did not exceed 1 mm/day. Using these simple procedures, tens of new single crystals of different organic materials were grown to cm-scale sizes with decent optical quality sufficient for the first tests of their properties for potential application in neutron detection. Examples of such crystals are shown in Figure 1.

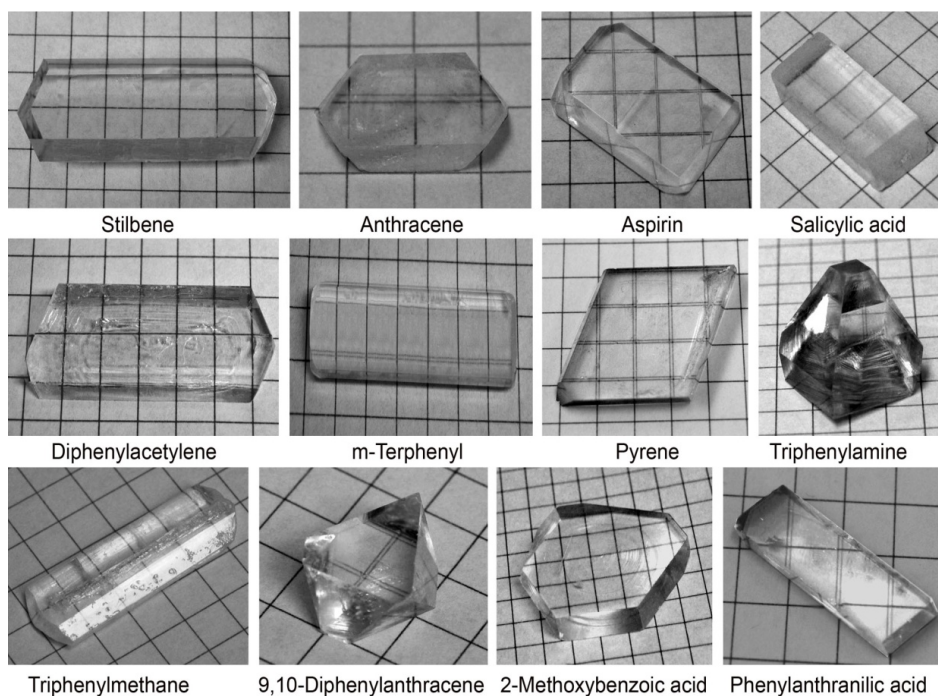


*Fig. 1. Organic single crystals grown by slow evaporation method. Size of the background square is 6.5 mm.*

Examination of multiple 3-PB crystals grown by the slow evaporation technique showed that the majority of the crystals formed in a simple shape consisting on the combination of a right hexagonal prism with two domes on its top and bottom, with  $105^\circ$  between two sides of the domes (Figure 2A). Additional small-area facets were observed in a few selected crystals, indicating that this typical simple shape shown in Figure 2B was not the full equilibrium shape of 3-PB, and more complicated faceting could develop under different conditions of growth. All

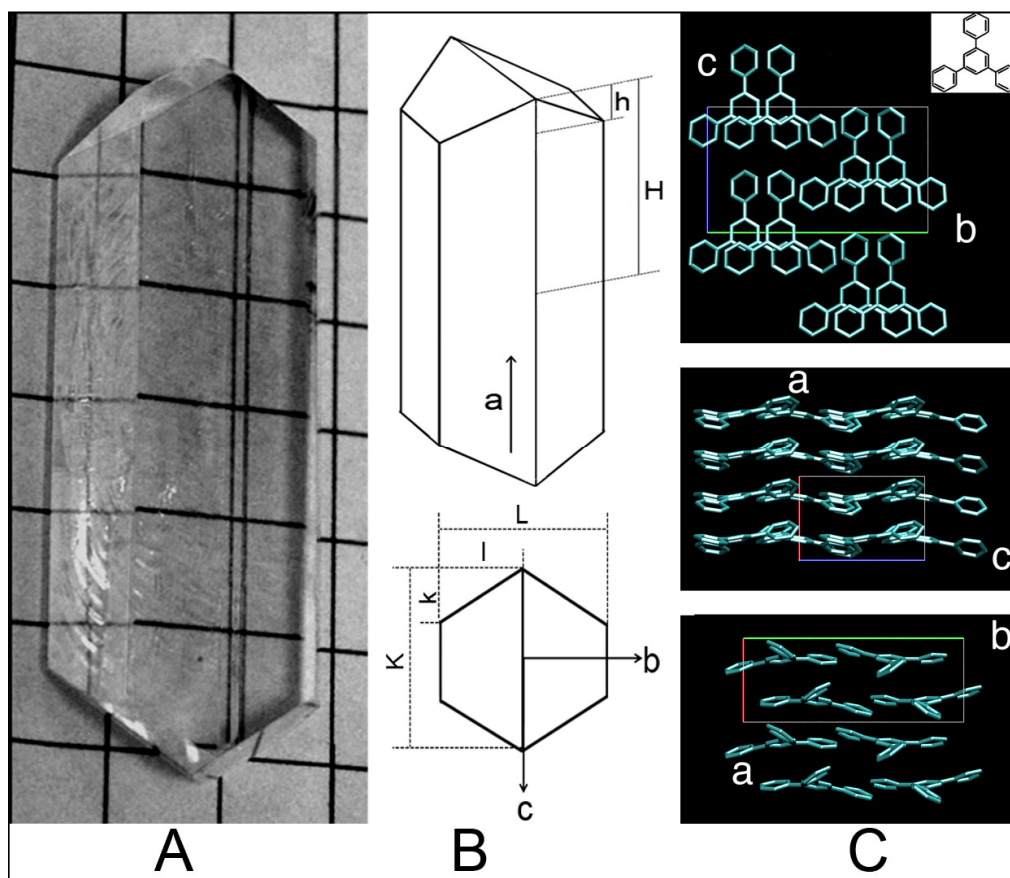


*Fig. 2. (A) 1,3,5-Triphenylbenzene crystal grown by slow evaporation method from toluene solution; the vertical size of the crystal is 42 mm. (B) schematic showing the most common facets formed in toluene solution; a, b, and c indicate the directions of crystallographic axes; other letters mark the sizes measured during rapid crystal growth. (C) Arrangement of the molecules in  $Pna2_1$  space group crystallographic lattice reconstructed from the data of Ref.11. Right upper insert shows an individual molecule structure.*

crystals had a well pronounced cleavage in the planes perpendicular to the long axis of the crystal. Previous studies [11] reported that 1,3,5-triphenylbenzene crystallizes in an orthorhombic structure with the symmetry class ( $mm2$ ) and space group  $Pna2_1$ . The existence of the cleavage planes was explained by the layered arrangements of almost planar molecules in the crystal lattice (Figure 2C). The fact that the orientation of the cleavage planes was found to be perpendicular to the a-direction of the lattice allowed for the positioning of the crystallographic axes in the grown crystals shown in Figure 2. Crystal density was measured using a commercial picnometer as  $1.14 \text{ g/cm}^3$ , which is smaller than the density reported previously for a collection of small crystals ( $1.221 \text{ g/cm}^3$ ) [11]. Established shape geometry and density were used for calculation of the crystal volume and mass during the rapid growth by temperature reduction method.

### ***3.2. Rapid growth by temperature reduction***

The major condition that prevents growth of larger crystals by the simple slow evaporation technique is the absence of solution stirring. Natural flow convection in a stagnant solution does not allow for a sufficient and uniform supply of crystallizing material to the surface of the growing crystal resulting in a diffusional regime of growth that may proceed without rough defect formation only at small crystal sizes and extremely slow growth rates [4].

A well established temperature reduction technique developed previously for rapid growth of KDP-type materials [5, 12] was used to obtain larger and better-quality 3-PB crystals. In this technique, a Pyrex crystallizer with growth solution of about 2.5 L in volume was placed in an external water bath used for thermostabilization with an accuracy of  $0.05^\circ\text{C}$ . All

controlling equipment, such as stirrers, heaters, coolers and thermocouples, were located outside the crystallizer to keep the growth solution in minimum contact with parts of the equipment. Although the crystallizer design was almost identical to that used previously for KDP-type crystals [6], some changes had to be introduced because of the use of organic chemicals.

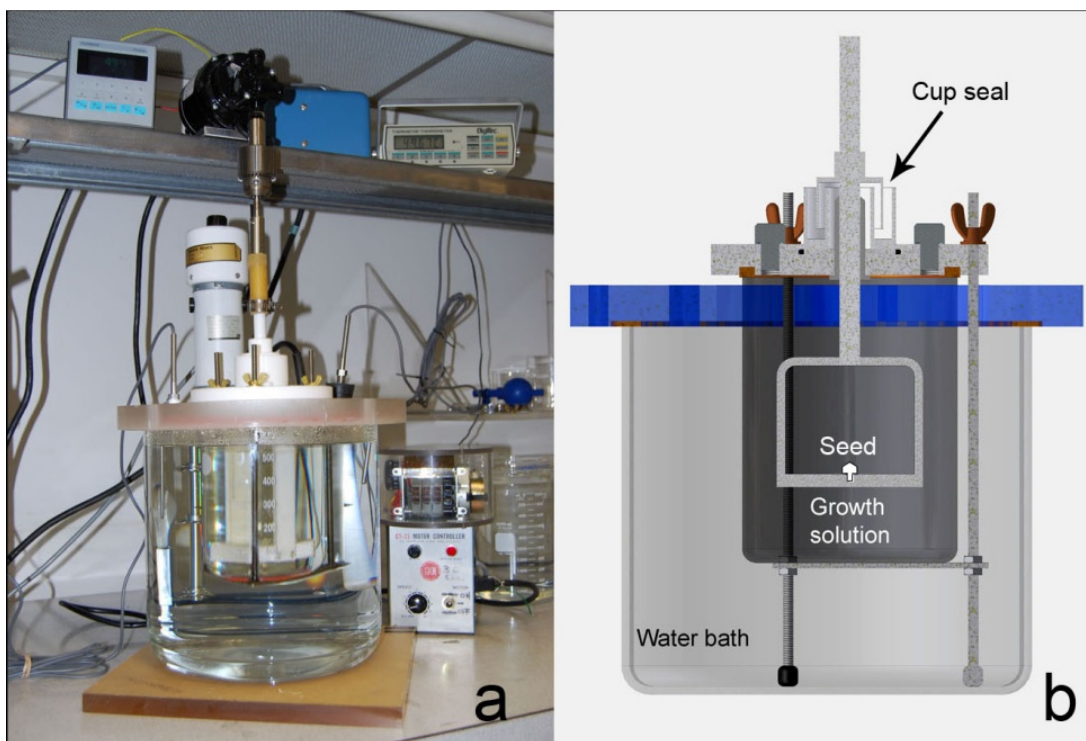


*Fig. 3. Photo (a) and general schematic (b) of a crystallizer used for crystal growth*

Different plastics, such as cast acrylic (Lucite) that can easily tolerate water solutions could not be used in the more chemically aggressive solvent, toluene. More inert Teflon was found to be an inappropriate material to replace these plastics because of its softness, easy deformation in heated toluene, and the porous nature that greatly diminished the stability of solutions to spontaneous nucleation initiated in the pores at lower supersaturation compared to the bulk of solution. Better results were obtained with stiffer and more resistant nylon that was used for

platform, stirrer and lid manufacturing. Since the design of a sealed crystallizer is essential for controlling the growth parameters during rapid growth, some modifications of the lid cup seal were made to reach better solution hermetization to prevent easy toluene evaporation that may lead to drying surfaces causing spontaneous nucleation during growth. With the same goal of toluene evaporation prevention, the solutions were transferred in and out the vessels only using chemically resistant tubing. These precautions in handling toluene without its exposure to air were also a part of the safety precautions required to work with flammable and hazardous materials.

In low-temperature solution growth, the relative supersaturation is the most important parameter to maintain for obtaining a desirable growth rate. It is typically defined as  $\sigma = (C - C_0)/C_0$ , where  $C$  and  $C_0$  are real and equilibrium (solubility) concentrations in the growth solution. In common practice of slow growth by temperature reduction,  $\sigma > 0$  required for crystal growth is typically created by an approximately estimated temperature drop that gradually increases with the crystal size. However, in rapid growth, large fluctuations in the growth rate produced by an arbitrarily chosen temperature reduction may cause formation of rough crystal defects accompanied by spontaneous nucleation. Much better control can be achieved by the monitoring of the supersaturation,  $\sigma$ , that takes into account both solubility,  $C_0$ , and gradually increasing crystal mass,  $M$ , at any given temperature,  $t$ , of the growth process:

$$\sigma = \left( \frac{PC_0(t_0) - M}{C_0(t)(P - M)} - 1 \right) 100\%, \quad (1)$$

where  $P$  is the weight of the initial growth solution saturated for the temperature  $t_0$ .

To obtain the values of 3-PB solubility in toluene, solutions containing solid powder were stirred at a constant temperature in a sealed crystallizer for 1-2 days. The equilibrium concentration  $C_0$  (Figure 4) was determined by a standard method of weighing solution samples before and after drying to a constant weight. Because of a possible sublimation of the powder at

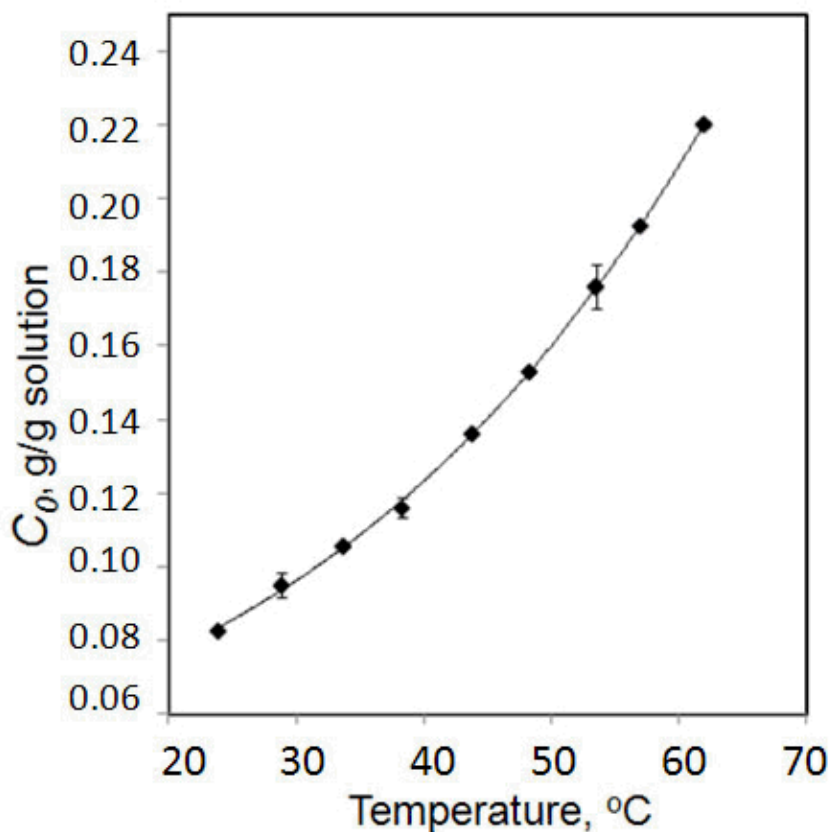


*Fig. 4. Temperature dependence of 1,3,5-triphenylbenzene solubility in toluene*

the drying temperatures, the data were verified by additional measurements in sealed solutions of known concentrations through the determination of the temperature at which a piece of a crystal could remain without growth or dissolution for some extended time. The results were approximated by an exponential equation  $C_0 = 0.0448e^{0.0255t}$  used to calculate  $C_0$  at intermediate temperatures in the measured range. Using the solubility data, solutions could be prepared with a

desired saturation temperature, typically chosen in the range of 50-55°C. The growth solution was filtered and left to overheat for a few hours at 10-15°C above the saturation point in a crystallizer with a stirrer connected to the rotation mechanism to provide reversible rotation of 50-60 rpm with a 15 second period in each direction, the same as the rotation used during crystal growth.

A seed with a vertical position of the long axis was cut from a crystal previously grown by the slow evaporation technique. It was glued to a platform so that the epoxy glue contacted only its leg, placed in a hole in the middle of the platform. As described previously [13], this method of binding noticeably decreases the probability of spontaneous nucleation and defect formation during the seed regeneration process. The platform with the seed was assembled in an empty crystallizer and slowly heated to a temperature about 5-7°C higher than the saturation point. Before the growth solution cooled to the same temperature, it was introduced into the crystallizer. The stirred solution with the seed was then allowed to cool to its saturation temperature to start the growth process.

The initial regeneration of the slightly dissolved seed was conducted at  $\sigma$  about 5% ( $\sim 2^\circ\text{C}$  below the saturation point of 55°C), which then was gradually increased to about 10% by the end of growth. Crystal dimensions were measured once a day. A special telescopic device was used for the measurements of the vertical size. To measure horizontal dimensions, a rectangular set of 5 mm-spaced grids were made on the platform surface. Lack of formation of additional facets except for those shown in Figure 2 resulted in a symmetrical shape of crystals allowed for a simplified crystal volume calculation based on its geometry as a combination of a hexagonal prism and a two-side dome. A semi-empirical formula obtained from the assumption of a perfect mirror symmetry of the crystal relatively to the (010) and (001) planes crossing in its center

$$M = \rho (KL - 2kl) (H - 0.37h) \quad (2)$$

made it possible to calculate crystal mass with the accuracy to a few percent. In this formula,

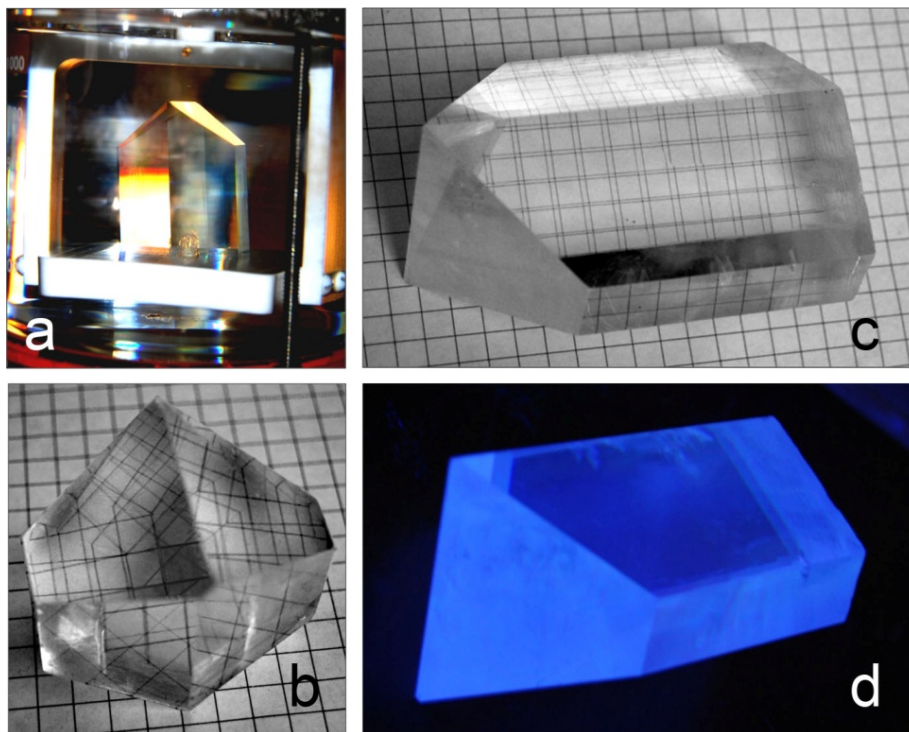


*Fig. 5. 1,3,5-triphenylbenzene single crystals: (a) during growth; (b) and (c) after growth with respective sizes of 60x55x41(mm) and 86x70x5 (mm) along the crystallographic directions; (d) picture taken under the UV-illumination.*

$\rho$  is the crystal density and the other parameters are the measured sizes shown in Figure 2b. It is obvious that with very non-uniform growth rates of different facets and less symmetric shapes, the calculations of the crystal volumes can require more precise and complicated formulas. Growth rates, mass and supersaturation were calculated immediately after the measurements. To obtain the value of the temperature drop, the next-day mass of the crystal was estimated based on its current growth rates. This expected mass and slightly increased supersaturation were used to calculate  $C_0(t)$  and a corresponding temperature from the solubility equation. Using the described

procedures, the first 3-PB crystals shown in Figure 5 were grown to the relatively large sizes close to 10 cm. Although the constant growth rate  $R_a$  of about 10 mm/day was intended to be kept, some fluctuation resulted in few minor solution inclusions occurred due to the lack of knowledge of  $R(\sigma, t)$  dependences, similar to those used to control KDP growth rates at decreasing temperature [6]. It should also be noted that despite the fact that practically the same crystallizer system design was used, precipitation of spontaneous crystals was observed more frequently than in the case of water soluble crystals. The problems show that further efforts are needed to improve the process. However, the overall results of the first experiments support the idea that solution growth methods can be successfully used to produce large volumes of organic scintillators for the use in neutron detection.

### ***3.3. Neutron detection properties***

Similar to many other crystals of aromatic compounds, 3-PB has fluorescence properties (Figures 5d and 6a), which determine its potential application as a scintillator material. A specific feature of some organic scintillators is that, in addition to the main scintillation component decaying exponentially (prompt fluorescence), they exhibit a delayed emission that decays at the same peak energy, but longer decay times [9]. The two-decay fluorescence was first demonstrated and developed using single organic crystals of anthracene, trans-stilbene, and p-terphenyl [14]. According to a commonly accepted mechanism [15, 16], the slow component that determines the PSD phenomena originates from the collisional interaction of pairs of molecules (or excitons) in the lowest excited triplet state  $T_1$ , while the fast component originates from the direct radiative de-excitation of excited singlets  $S_1$ . Since triplets are known to be

mobile in some compounds, the energy migrates until two triplets collide and experience an Auger up-conversion process:  $T_1 + T_1 \rightarrow S_0 + S_1$ . The enhanced level of delayed emission for neutrons arises from the short range of the energetic protons produced from neutron collisions (thereby yielding a high concentration of triplets), compared to the longer range of the electrons from the gamma interactions, giving rise to pulse shape discrimination (PSD) properties of organic scintillators used for the detection of high-energy neutrons in the presence of gamma radiation.

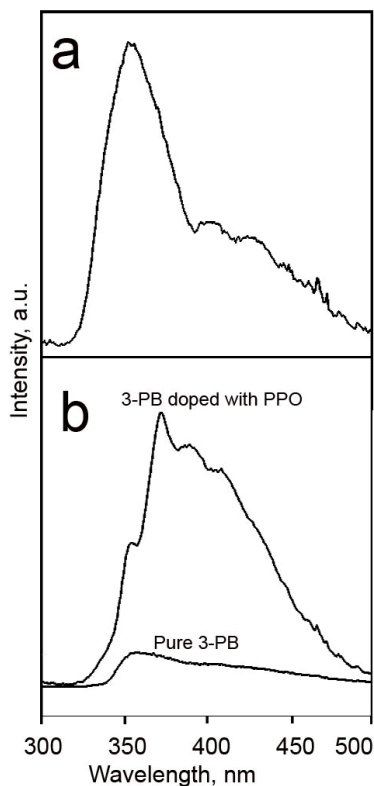


*Fig. 6. (a) Emission spectrum of 1,3,5-triphenylbenzene single crystal; (b) Comparative intensity of photoluminescence obtained with a pure and a PPO-doped 1,3,5-triphenylbenzene crystals measured under the same conditions. Excitation wavelength – 273 nm.*

Major developments in understanding these properties have been made with trans-stilbene single crystals, an efficient PSD material used for decades as a standard for comparison with other solid and liquid organic scintillators. Recent availability of high-speed waveform

digitizers greatly simplified processing of gamma-neutron signals [17-19], enabling us to conduct much broader studies of many new materials, among which 3-PB was one of the first crystals [20] with the PSD properties that could be potentially used in neutron detection.

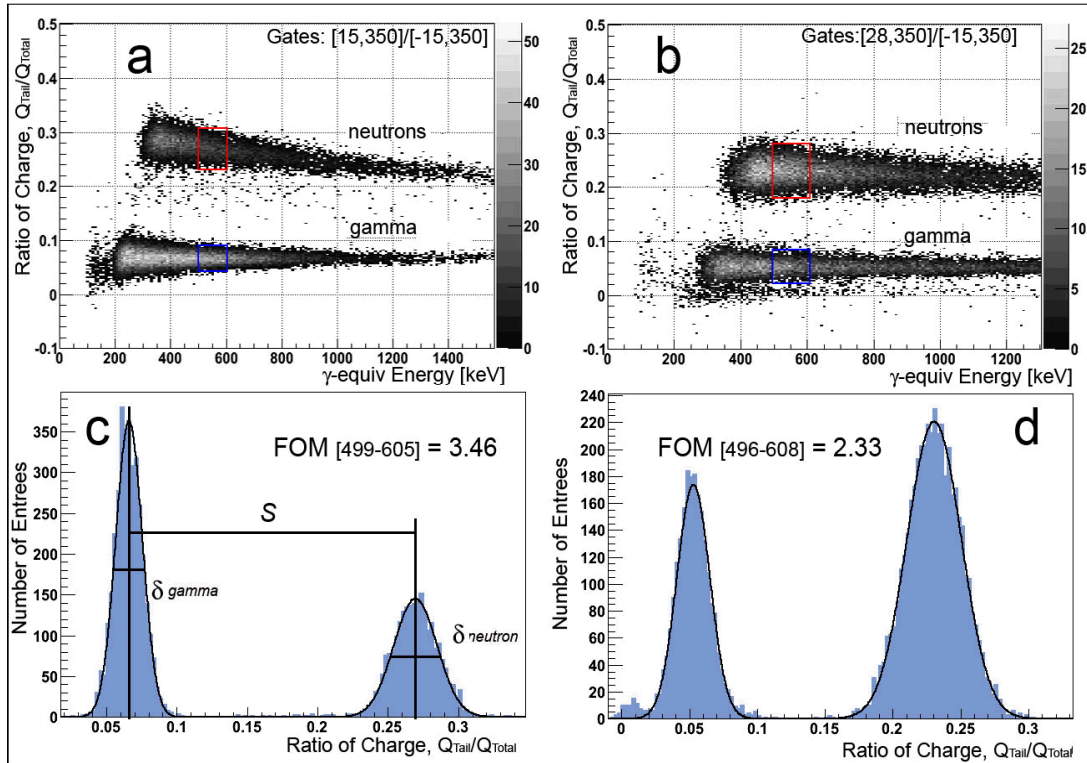


Fig. 7. (a and b) - Neutron-gamma PSD pattern obtained with stilbene and 3-PB crystals, respectively; rectangles indicate regions used for composite waveform and FOM. (c and d) - PSD profiles for the calculation of Figures of Merit of stilbene and 3-PB crystals, respectively.  $^{252}\text{Cf}$  source used in all measurements. Energy scales were calibrated using the Compton edge from  $^{137}\text{Cs}$ .

PSD measurements made in the present work with numerous 3-PB crystals always revealed a good level of neutron-to-gamma discrimination with a neutron-to-gamma peak separation similar to that obtained with stilbene crystals (Figure 7, a and b). More precise evaluation of the potential PSD performance of the new material was made by comparison to stilbene using typical calculations of the figures of merit *FOM*

$$FOM = \frac{S}{\delta_{neutron} + \delta_{gamma}}, \quad (3)$$

which take into account not only the separation between neutron and gamma peaks  $S$ , but also the width of the peaks  $\delta$  (Figure 7e). As seen from the results shown in Figure 7, c and d, the calculated FOMs give smaller value for 3-PB compared to that of the stilbene crystal. The reason for the difference originate from much broader scatter of the individual points in the 3-PB pattern partially related to much lower intensity of the fluorescence pulses typical for all 3-PB crystals. Measurements of the beta-induced scintillation light yield showed more than four times lower values for 3-PB crystals in comparison to stilbene (about 6000 Ph/MeV vs 25000 Ph/MeV). Full characterization of materials for neutron detection will require measurement of the neutron quench factor, the ratio of the response to recoil protons and to electrons, to better relate gamma-equivalent energy to neutron energy. The relatively low scintillation efficiency decreases chances of 3-PB to become a wide-spread material for neutron detection. There is, however, a possibility that further research may help overcome this inadequacy. Our recent studies show that the small addition of bright fluorophores, such as stilbene, diphenylbutadiene and 2,5-diphenyloxazole (PPO) (Figure 6 b) may result in a substantial increase of the luminescence intensity and scintillation light yield, opening broader opportunities for the practical use of this new material.

### ***3.4. Model comparison of PSD in different organic scintillators***

Growth of the first 3-PB crystals gives reasonable hopes that many of new organic compounds tested for their neutron detection properties at small sizes, similar to those shown in

Figure 1, will be grown at a scale needed for their practical application. The availability of a large number of new crystals opens first opportunities for studies of the PSD phenomena in different types of organic materials. One of the tasks needed to initiate such studies is identification of the PSD process parameters that, being attributed to the specific properties, such as chemical composition, molecular and crystallographic structure, etc., can be used for the comparison, selection and engineering of new materials.

In this work, we have implemented a model that describes the gamma and neutron response of our 3-PB and trans-stilbene samples. The model is based on a simple physical picture where singlet and triplet excited state populations evolve from their initial concentrations,  $N$ , *via* the governing equations,

$$dN_{\text{singlet}}/dt = -N_{\text{singlet}}/\tau_{\text{singlet}} + \gamma N_{\text{triplet}}^2 \quad (4)$$

$$dN_{\text{triplet}}/dt = -N_{\text{triplet}}/\tau_{\text{triplet}} - 2\gamma N_{\text{triplet}}^2, \quad (5)$$

where the Auger up-conversion ( $\gamma$ ) and the excitation lifetimes ( $\tau_{\text{singlet}}$  and  $\tau_{\text{triplet}}$ ) are assumed to be the same for the gamma and neutron response. We define the initial triplet concentration for the neutron response to be 1, and other concentrations are measured relative to  $N_{\text{triplet}}^0$ . A simultaneous fit of the gamma and neutron peak normalized composite response waveforms is performed using a  $\chi^2$  minimization routine; the resulting fits are shown in Figure 8. We have added a fixed percentage error, 4% for 3-PB and 9% for stilbene, in quadrature with the statistical error for each point to obtain a  $\chi^2$  per degrees of freedom of approximately 1. This may give a rough estimate of unaddressed system effects like PMT characteristics and resolution for determining the peak time of individual pulses. The use of single photon counting from a loosely coupled fiber to construct waveforms may be used in future work to reduce such system effects.

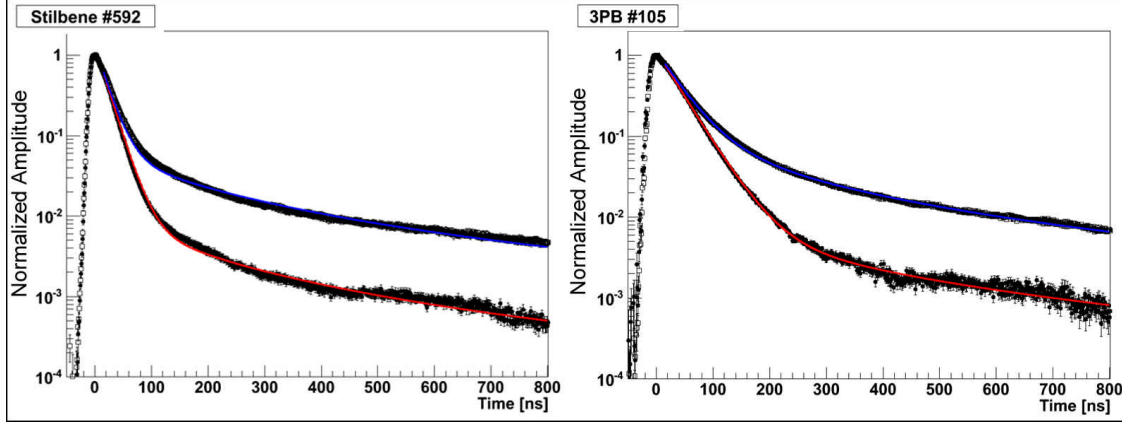


Figure 8. Peak normalized composite waveforms of the response to gamma (lower curves) and neutron (upper curves) stimulations for stilbene (left) and 3-PB (right) samples. The solid curves are best fits from the model described in the main text. The error bars are the quadrature sum of statistical and a fixed percentage error as described in the text.

We note that reasonable fits require  $\tau_{\text{triplet}} \gg \tau_{\text{singlet}}$ , making the model insensitive to its value.

We also found that allowing a fraction of the singlet population to transfer to the triplet population failed to produce reasonable fits for meaningful parameter values. This result shows that formation of the excited triplet states occurs by the direct excitation, rather than *via* the intersystem crossing by the nonradiative relaxation of singlets. The parameter values from the best fits for the 3-PB and stilbene samples are presented in Table 1.

Table 1. Fitted parameters from the model described in the main text to composite waveforms shown in Fig. XX for the gamma and neutron stimulations of 3-PB and stilbene.

Material		$N_{\text{triplet}}^0$	$N_{\text{singlet}}^0$	$N_{\text{triplet}}^0/N_{\text{singlet}}^0$	$\tau_{\text{singlet}}$	$\gamma$
Triphenylbenzene	Gamma	0.87	5.3	0.16	38	0.002
	Neutron	1.0 (fixed)	0.71	1.4		
Stilbene	Gamma	1.3	5.4	0.24	19	0.0018
	Neutron	1.0 (fixed)	0.57	1.7		

For both materials, the model indicates that triplets are a small fraction of all initial excitations for the gamma response. However, the initial triplet excitations significantly exceed singlets for the neutron response. The change from gamma to neutron stimulation response is primarily due to a large decrease in singlet concentration, although triplet concentration shows some increase for 3-PB compared to a drop for stilbene. The extracted singlet lifetime ( $\tau_{\text{singlet}}$ ) varies by roughly a factor of two while the Auger up-conversion parameter ( $\gamma$ ) appears similar for both materials; however, the fitted value of  $\gamma$  for stilbene is noticeably dependent on how far the fit range extends into the tail.

Since the ratio of delayed luminescence to total luminescence is a standard PSD discriminate, a neutron response where: (1) triplet excitations dominate the initial population, (2) singlet excitations decay quickly, and (3) triplet excitations slowly create singlet excitations, may prove ideal. Using variations of the model parameters around those of 3-PB to estimate their relationship with the  $R_{\text{neutron}} - R_{\text{gamma}}$ , where  $R = Q_{\text{Tail}}/Q_{\text{Total}}$  is the gate optimized neutron-gamma separation discriminate, we find that  $(N_{\text{triplet}}^0)^{0.61}/[(N_{\text{singlet}}^0)^{0.68}\gamma^{0.14}(\tau_{\text{singlet}})^{0.20}] \equiv M$  estimates the dependence of  $M_{\text{neutron}} - M_{\text{gamma}}$ . This indicates the initial singlet and triplet concentrations are of the most, and roughly equal, importance. There is a weaker dependence on the singlet lifetime, and the weakest dependence is for the Auger up-conversion parameter. These results are for the limit of an acquisition system with infinite integration time and no noise, but the model can provide insight into more realistic cases. For a system with a 500 ns integration time, our model suggests that  $\gamma \approx 0.0027$  is best for a material otherwise like 3-PB. We note that fluctuations in the PSD discriminate variable, which give rise to FWHM terms in the FOM calculation Eqn. 3, are not fully reflected in this study of averaged waveforms. Other practical considerations such as digitizer speed and pileup avoidance in high rate environments

will also impact the results of analysis. However, we believe that further development of the model will provide physical insight into the processes relevant to producing the delayed luminescence essential to PSD, and will be useful for comparison and possibly prediction of goodness of materials for PSD based neutron detectors.

## **Conclusion**

Faceted single crystals of a pure hydrocarbon, 1,3,5-triphenylbenzene, were grown from toluene solutions by the temperature reduction method. Good optical quality and relatively high growth rates, up to 10 mm/day, obtained in the absence of spontaneous nucleation from solutions show that the rapid growth technique developed previously for growth of large inorganic crystals from aqueous solutions can be applied to pure organic systems. Characterization of the physical properties showed that 1,3,5-triphenylbenzene can be potentially used as a scintillator for high-energy neutron detection in the presence of gamma radiation background. Successful growth of this crystal opens a pathway for comparative studies of the PSD phenomena in different types of organic materials and large-volume production of more efficient scintillators for high-energy neutron detection.

## **Acknowledgement**

This work was performed under the auspices of the U.S. Department of Energy by Lawrence Livermore National Laboratory under Contract DE-AC52-07NA27344 and supported by the U.S. Department of Energy Office of Nonproliferation Research and Development (NA-22).

## References

1. Nyvit and Soehnel, *The Kinetics of Industrial Crystallization*, Elsevier Amsterdam (1985).
2. A. S. Myerson, *Handbook of Industrial Crystallization*, Butterworths: Montvale, MA , (1992).
3. A. McPherson, *Preparation and Analysis of Proteins Crystals*, John Wiley & Sons, New York (1982).
4. L.N. Rashkovich, *KDP Family of Crystals*, Hilger-Bristol (1991).
5. N.P. Zaitseva, J.J. De Yoreo, M.R. Dehaven, R.L. Vital, K.E. Montgomery, M. Richardson, L.J. Atherton, *J. Cryst. Growth* **180** (1997) 255-262.
6. N.Zaitseva, L.Carman, Rapid growth of KDP and DKDP crystals, *Progress of Crystal Growth and Characterization of Materials* **43** (2001) 1-118
7. V.I. Bredikhin, G.L. Galushkina, V.P. Ershov, V.I. Rubakha and N.R. Shvetsova, *J. Cryst. Growth* **207** (1999) 122-126.
8. N.P.Zaitseva I.L.Smolsky L.N.Rashkovich, *Soviet Physics Crystallography*, V.36, 113-115 (1991).
9. Birks, J.B., *The Theory and Practice of Scintillation Counting*, Pergamon Press, London (1964).
10. Brooks, F.D., *Nucl. Instr. Methods* **162**, (1979) 477-505.
11. M.Shehata Farag, *Acta Cryst.* (1954) **7**, 117-120
12. N.P.Zaitseva, L.N.Rashkovich, S.V.Bogatyreva, *J.Cryst. Growth* **148** (1995) 276-272
13. N.Zaitseva, I.Smolsky, and L.Carman, *J.Cryst.Growth*, **241** (2002), 363-373.
14. Wright, G.T., *Proc.Phys.Soc.* **B69**, 1956, 358-372.
15. Brooks, F.D., *Nucl. Instr. Methods* **4**, 1959, 151-163.
16. Brooks, F.D., *Nucl. Instr. & Meth.*, **162**, 1979, 477-505.
17. Jastaniah, S.D. and Sellin, P.J., *IEEE Trans. Nucl. Sci.*, **49**, 2002, 1824-1828.

18. Kaschuck Y.; Esposito, B., *Nucl. Instr. & Meth. A*, **551**, 2005, 420-428.
19. N. V. Kornilov, V. A. Khriatchkov, M. Dunaev, A. B. Kagalenko, N. N. Semenova, V. G. Demenkov, and A. J. Plompen, *Nucl. Instr. and Meth. A*, **497**, 2003, 467-478.
20. G.Hull, N.Zaitseva, N.Cherepy, J.Newby, W.Stoeffl, and S.Payne, *IEEE Transactions on Nuclear Science* **56**, 2009, 899-903.